УДК 303.732.4
DOI: 10.26102/2310-6018/2026.54.3.021

Signal-based feature extraction in motor evoked potentials: TKEO onset detection and Hilbert envelope analysis

Y. Demigha[1]✉, E.V. Lyapuntsova[1,2]

[1]National Research University of Technology "MISIS", Moscow, the Russian Federation
[2]Bauman Moscow State Technical University, Moscow, the Russian Federation

Abstract. The reliable and objective determination of the characteristics of the motor evoked potential (MEP) – latency of occurrence, amplitude from peak to peak, duration and morphology of the waveform – is fundamental for clinical neurophysiology, but in modern practice it largely depends on the judgments of the operator. Mathematical algorithms for signal processing offer a transparent, deterministic and reproducible alternative. We present, characterize, and systematically evaluate a complete mathematical algorithm for identifying MEP features, consisting of three stages: determining the origin based on TKEO, the Tiger-Kaiser energy operator applied to a pre-processed signal with an adaptive threshold $k \cdot \sigma\_baseline$; Estimating the displacement of the Hilbert transform – amplitude envelope tracking using a baseline return criterion; and morphological classification by counting significant zero crossings to assign monophase, two-phase, or multiphase labels. At the marker verification stage, tests in which the detected signs do not exceed the minimum noise level are rejected. With an SNR value of 3.0, performance decrease, the MAE delay increases from 1.4 ms (SNR ≥ 5) to 9.7 ms (SNR < 3). The accuracy of morphological classification is 94% for studies with high SNR and decreases to 61% for studies with very low SNR. The mathematical pipeline provides clinically acceptable accuracy for MEP with high and medium SNR levels and serves as an interpretable reference standard with zero training costs. Its failure modes are well characterized, SNR-dependent, and predictable – properties that make it a basic baseline comparator for evaluating more advanced automated analysis methods.

Keywords: motor evoked potentials, transcranial magnetic stimulation, TKEO, Tiger-Kaiser energy operator, Hilbert transform, amplitude envelope, electromyography, signal processing.

For citation: Y. Demigha, Lyapuntsova E.V. Signal-based feature extraction in motor evoked potentials: TKEO onset detection and Hilbert envelope analysis. *Optimization and Information Technology*. 2026;14(3). URL: https://moitvivt.ru/ru/journal/article?id=2294 DOI: 10.26102/2310-6018/2026.54.3.021

Выделение признаков на основе сигналов в моторных вызванных потенциалах: обнаружение возникновения TKEO и анализ гильбертовой огибающей

Ю. Демига[1]✉, Е.В. Ляпунцова[1,2]

[1]Национальный исследовательский технологический университет «МИСИС», Москва, Российская Федерация
[2]Московский государственный технический университет имени Н.Э. Баумана, Москва, Российская Федерация

Резюме. Надежное и объективное определение характеристик моторного вызванного потенциала (МВП) – латентности возникновения, амплитуды от пика до пика, длительности и морфологии волновой формы – имеет фундаментальное значение для клинической нейрофизиологии, но в

современной практике оно во многом зависит от суждений оператора. Математические алгоритмы обработки сигналов предлагают прозрачную, детерминированную и воспроизводимую альтернативу. Мы представляем, описываем и систематически оцениваем полный математический алгоритм для идентификации характеристик МВП, состоящий из трех этапов: определение начала координат на основе TKEO, оператора энергии Тайгера-Кайзера, применяемого к предварительно обработанному сигналу с адаптивным порогом $k \cdot \sigma\_baseline$; оценка смещения преобразования Гильберта – отслеживание амплитудной огибающей с использованием критерия возврата к базовой линии; и морфологическая классификация путем подсчета значимых пересечений нуля для присвоения меток монофазного, двухфазного или многофазного сигнала. На этапе проверки маркеров отклоняются тесты, в которых обнаруженные признаки не превышают минимальный уровень шума. При значении SNR, равном 3,0, производительность снижается, а задержка MAE увеличивается с 1,4 мс (SNR ≥ 5) до 9,7 мс (SNR < 3). Точность морфологической классификации составляет 94% для исследований с высоким SNR и снижается до 61% для исследований с очень низким SNR. Математический алгоритм обеспечивает клинически приемлемую точность для MEP при высоком и среднем уровнях SNR и служит интерпретируемым эталонным стандартом с нулевыми затратами на обучение. Его режимы отказов хорошо охарактеризованы, зависят от SNR и предсказуемы – свойства, которые делают его базовым компаратором для оценки более продвинутых методов автоматизированного анализа.

Ключевые слова: моторные вызванные потенциалы, транскраниальная магнитная стимуляция, TKEO, энергетический оператор Тигера-Кайзера, преобразование Гильберта, амплитудная огибающая, электромиография, обработка сигналов.

Для цитирования: Ю. Демига, Ляпунцова Е.В. Выделение признаков на основе сигналов в моторных вызванных потенциалах: обнаружение возникновения TKEO и анализ гильбертовой огибающей. *Моделирование, оптимизация и информационные технологии.* 2026;14(3). (На англ.). URL: https://moitvivt.ru/ru/journal/article?id=2294 DOI: 10.26102/2310-6018/2026.54.3.021

Introduction

Motor evoked potentials (MEP) are short-term electrical reactions recorded by peripheral muscles after stimulation of the cerebral cortex, most often using transcranial magnetic stimulation (TMS). They are the primary non-invasive method for determining the functional integrity, excitability, and speed of the spinal cord velocity [1]. Three quantitative parameters are usually extracted from each MEP study: latency of onset (the interval from the supply of a stimulus to the first deviation of the EMG from the background, reflecting the speed of the motor conduction cortex, usually 20–45 ms for the muscles of the upper extremities [2]); the amplitude from peak to peak (the difference in voltage between the positive and negative peaks of the reaction, reflecting the size and synchronicity of the involved pool of motor neurons, varies from tens of mv in patients with disorders to several μV in healthy subjects [3]); and duration (the interval from the beginning to the end of the reaction). the return of the signal to the noise level reflecting the temporal dispersion of the descending corticospinal pulse, usually 15–80 ms [4]). The fourth descriptor – the morphology of the waveform (monophasic, biphasic, or polyphasic), provides qualitative information about the structure of the set and is used to check the quality of responses before quantitative analysis [3].

Despite its central role in clinical practice, in the vast majority of clinical and research processes, MEP functions are extracted manually. The operator visually determines the origin, peaks, and offset on the visualized waveform graph, usually using the cursor. This approach suffers from several well-documented limitations: the interclass variability of a 2–8 ms latency [5], a subjective amplitude threshold that is inconsistent between trials with different levels of background activity, and bandwidth limitations that become prohibitive in large study datasets

(5,000–50,000 trials per multi-session study). In addition, the lack of a documented, reproducible decision-making rule makes it difficult to compare measurement results in different laboratories or clinical centres [1].

Signal processing methods offer a deterministic, operator-independent alternative to manual extraction. The task of automated MEP detection is to distinguish a short-term increase in energy during the appearance of MEP from continuous background EMG noise. Two mathematical models proved to be particularly well suited for this task.

The Tiger-Kaiser energy operator (TKEO) was introduced by Kaiser [6] as a discrete approximation to the instantaneous mechanical energy of a signal: $\psi[x(n)] = x^2(n) - - x(n-1) \cdot x(n+2)$. Its key property is that it does not proportionally amplify the sudden increase in signal energy at once stationary and makes it a highly sensitive detector of transient processes such as MEP triggering. Skolnik et al. [7] demonstrated in a systematic review that TKEO-based start detection is superior to simple threshold and moving average methods for the EMG signal in a few numbers of SNR conditions.

To determine the offset, the Hilbert transform provides a continuous amplitude envelope of the signal using an analytical signal:

$$(t) \; = \; x(t) \; + \; j \cdot H[x(t)],$$

where $H[x(t)]$ denotes the Hilbert transform a $|z(t)|$ instantaneous amplitude envelope [6] the return of this envelope to the base level provides fundamentally phase-independent criteria for the displacement of the MEP, surpassing derivative-based methods that are sensitive to fluctuations caused by noise near the end of the response [8].

The classification of signal morphology by counting the intersection of zeros was used in needle EMG analysis [3] and is directly applicable to the classification of MEP. A significant zero crossing, such that the transition between positive and negative polarities occurs at a point where the signal exceeds $2x\sigma\_baseline$, means a genuine change in the polarity of the MEP, and not a fluctuation caused by noise.

In the present study, these three well-established mathematical methods are combined into a complete comprehensive analysis of the characteristics of MEP and, for the first time, a rigorous quantitative characterization of their overall accuracy, failure modes, and SNR dependencies are presented for five different participant response profiles. The specific goals are: the formal definition of each step of the algorithm with its mathematical derivation; the estimation of the delay, amplitude and duration of MAE in 200 synthetic trials; the determination of the accuracy of morphological classification by type of waveform and SNR; and identify the SNR limits below which mathematical analysis becomes unreliable, providing empirically sound recommendations for its proper clinical application.

Materials and methods

Overview of the mathematical pipeline the complete pipeline is shown in Figure 1. It consists of five consecutive stages: signal preprocessing, baseline noise level estimation, TKEO onset detection, peak detection with Hilbert shift estimation, and morphological classification. At the intermediate marker verification stage, tests are rejected if any detected marker does not exceed the baseline noise threshold.

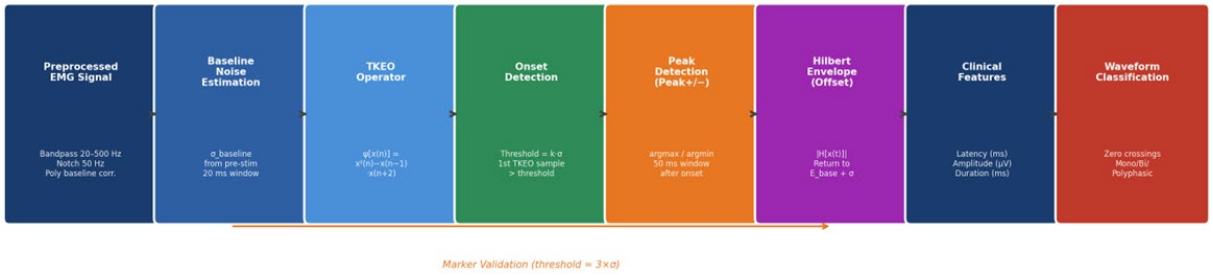

Figure 1 – A complete mathematical pipeline for identifying MEP features
Рисунок 1 – Полный математический конвейер выделения признаков МВП

Pre-processing of signals. Before identifying features, each EMG epoch goes through the following processing steps using SciPy [9]:

– Notch filter: a 2nd order notch IIR filter with a frequency of 50 Hz (Q = 30) to eliminate interference in the power line.

– Bandpass filter: a 5th order zero-phase Butterworth filter, 20–500 Hz (scipy.signal.filtfilt), which preserves the physiological range of EMG while eliminating DC bias.

– Fast polynomial correction: first order least squares polynomial corresponding to the segment preceding the (0–20) ms stimulus and subtracted from the full epoch to eliminate residual linear illumination without phase distortion.

Fast polynomial correction: first order least squares polynomial corresponding to the segment preceding the stimulus (0–20 ms) and subtracted from the full epoch to eliminate residual linear illumination without phase distortion.

All feature extraction algorithms work with a preprocessed signal, the pre-exposure window (the first 20 ms, 40 samples at a frequency of 2,000 Hz) serves as the base for all stages of noise assessment throughout the process.

Estimation of the baseline noise level the exact noise characteristic is the basis for each subsequent threshold value. For each test, the standard ignition of the initial noise level is calculated based on the segment preceding the stimulus.

$$\sigma\_baseline = std(x(t),\ for\ t \in [0, T\_stim]),$$

where $T\_stim = 20$ ms, and $x(t)$ denotes the preprocessed signal, three additional indicators are calculated for reporting and validation purposes, the basic and average quadratic indicator ($\sigma\_RMS = average\ quadratic\ value\ for\ the\ segment\ before\ stimulation$), the base range from peak to peak and the 95th percentile $|x(t)|$ for the period before stimulation, the latter provides me with a pair of metric estimates of the upper bound that is resistant to the right-skewed noise distribution documented in records of MEP [10]. Then the primary detection threshold is determined to be

$$Threshold = k \cdot \sigma_{baseline} \quad (default: k = 3.0).$$

This adaptive threshold is automatically scaled depending on the noise conditions of each study to ensure that the detection criteria are consistently calibrated regardless of the recording session of the subject or the variability of the equipment.

Detecting TKEO first

The Tigger-Kaiser energy operator. The Tehran-Kaiser energy operator with discrete time is defined as follows [6, 11].

$$\psi[x(n)] = x^2(n) - x(n-1) \cdot x(n+2).$$

For a sinusoidal signal $x(n) = A \cdot cos(\Omega \cdot n + \varphi)$ TKEO approximates the instantaneous energy as $A2 \cdot sin2(\Omega)$, by making it proportional to both the square of the amplitude and the squares of the purity, this double sensitivity is the source of its ability to recognize the beginning of the MEP, causing a sudden increase in both amplitude and frequency compared to background noise, which leads to a large sharply localized spike in the output signal. Its ticks at the beginning of the selection are on the contrary smooth, even with moderate amplitude noise creates a signal close to the number of neighboring samples strongly correlates with zero [7].

The adaptive algorithm for determining the threshold and the start of the TKEO start detection action is performed as follows:

– calculate TKEO and apply $\psi[\cdot]$ by the full preprocessing epoch to obtain the energy signal $\psi[x(n)]$;

– estimate the initial TKEO level and calculate $\sigma\_TKEO = std(\psi[x(n)])$ during the period preceding the stimulus ($n \in [0, T\_stim]$);

– set the threshold value to $Threshold\_TKEO = k \cdot \sigma\_TKEO$ (same scaling factor $k = 3.0$);

– forward iteration stimulus scan $n = T\_stim$; начальный индекс n_onset is the first sample, where $\psi[x(n)] > Threshold\_TKEO$;

– backup option if more than one sample does not exceed the threshold value and within the search window (from T_stim до $T\_stim + 150$ ms), the test is marked as unsuccessful, and the start is set to TKEO.

Figure 2 shows a detailed visualization of each stage, including the basic TKEO distribution, the detection zone and the sensitivity of the detection of the beginning of k to the scaling factor k. Panel E demonstrates that $k = 3.0$ provides a stable operating point for estimating the delay stable at $k \approx [2.5, 4.5]$ for signals with high SNRs but quickly diverge at lower values of k because caused by noise its tic spikes prematurely exceed the threshold value.

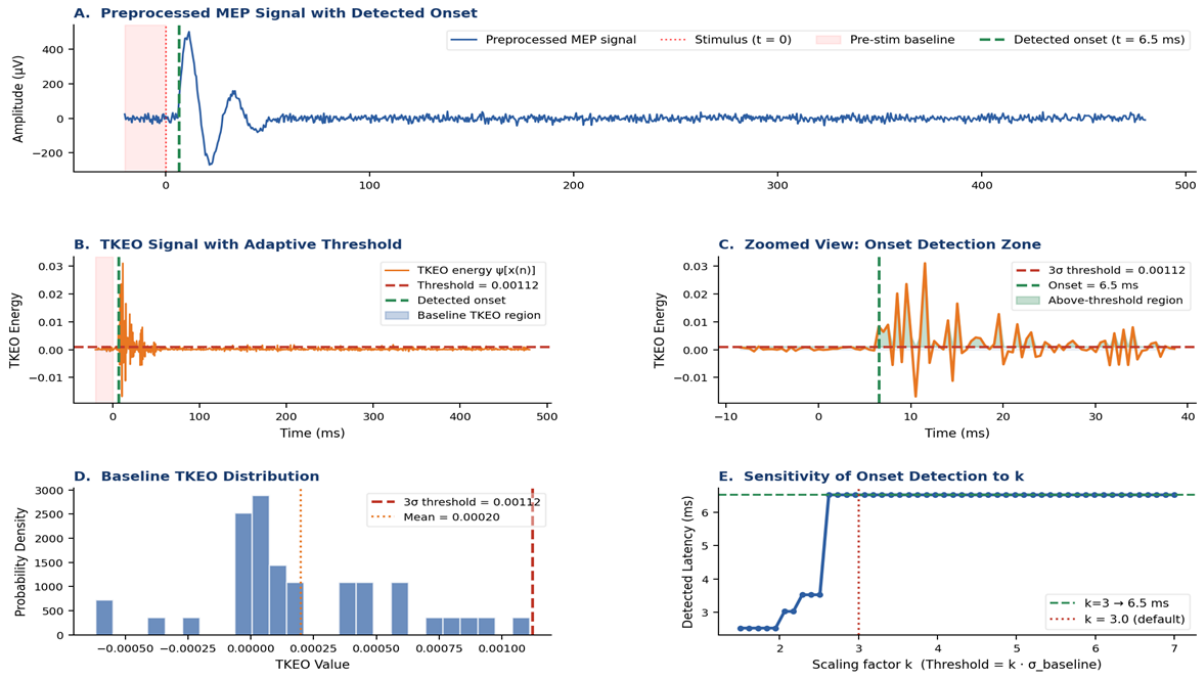

Figure 2 – Detection of the onset of MEP based on TKEO
Рисунок 2 – Обнаружение начала МВП на основе TKEO

Peak detection. Once the n_onset start index is set, peak detection continues for the 50-second search period immediately after the start:

$$n\_Peak+ = argmax\, x(n)\ for\ n \in [n\_onset, n\_onset + 0{,}05 \cdot fs],$$

$$n\_Peak- = argmin\, x(n)\ for\ n \in [n\_onset, n\_onset + 0{,}05 \cdot fs].$$

A 50 ms window captures the typical shape of the MEP signal for the muscles of the upper extremities (duration 15–80 ms [4]), excluding late polysynaptic components. The search for both peaks is carried out within the same window, since the two-phase nature of most MFPs means that positive and negative peaks are separated by only one zero crossing, usually within 20–40 ms. The following formula determines the peak-to-peak amplitude:

$$Amplitude = |x(n\_Peak+) - x(n\_Peak-)|.$$

Determining the offset of the Hilbert transform

Analytical signal and amplitude envelope. Displacement detection uses the Hilbert transform to calculate the envelope of the instantaneous amplitude of the signal [12]. The analytical signal has the form:

$$z(t) = x(t) + j \cdot H[x(t)],$$

where $H[\cdot]$ stands for the Hilbert transform. The instantaneous envelope of the amplitude is:

$$A(t) = |z(t)| = \sqrt{(x^2(t) + H[x(t)]^2)}.$$

The Hilbert transform is calculated from the analytical signal of a real signal using the FTT-based method (scipy.signal.hilbert [9]). Unlike the original signal, $A(t)$ is always non-negative and varies smoothly, making it immune to rapid fluctuations that interfere with derivative-based bias methods [8].

The offset detection algorithm first evaluates the basic envelope statistics:

$$\mu\_env = mean(\, A(t)\ for\ t < T\_stim\,),$$

$$\sigma\_env = std(\, A(t)\ for\ t < T\_stim\,).$$

The return threshold value is defined as как $\mu\_env + \sigma\_env$. The offset index is the first sample after the latter of the two peaks (n_Peak+, n_Peak-), when the envelope falls below this threshold value again:

$$n\_offset = The\ primary\ maximum\ value(n\_Peak+, n\_Peak-),$$

where $A(n) < \mu_{env} + \sigma_{env}$.

If no return is detected during the 200-millisecond search period, the offset is set to the end of the search period, and the trial version is marked. Figure 3 shows the components of the analytical signal, the envelope with threshold bands, and the final complete marker set for the signal.

Where A: The components of the analytical signal are the initial (blue), the quadrature component (orange dotted line) and the amplitude envelope (red). B: An envelope with a return threshold ($\mu\_env + \sigma\_env$), green dotted line) and a detected end (purple). Q: A complete set of markers on the MEP signal – start (▲), positive peak (●), negative peak (▼), end (■) – with duration annotation.

Calculation of clinical signs. After determining the 4 marker indices, the 3 clinical signs are calculated as follows:

$$Latency\ (ms) = n\_onset\ /\ fs \cdot 1000,$$

$$Amplitude(\mu V) = |x(n\_Peak+) - x(n\_Peak-)| \cdot 10^6,$$

$$Duration\ (ms) = (n\_offset - n\_onset)\ /\ fs \cdot 1000.$$

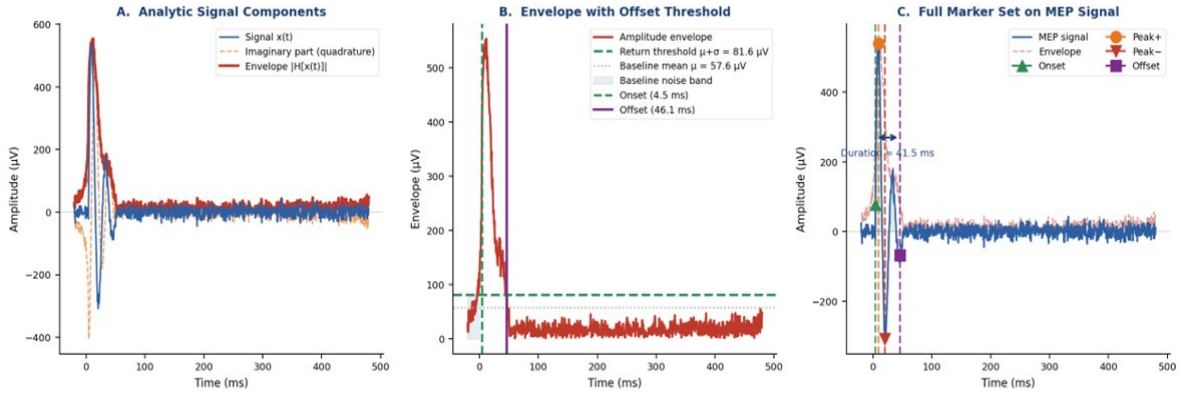

Figure 3 – MEP offset detection via Hilbert transform amplitude envelope
Рисунок 3 – Определение смещения МВП с помощью огибающей амплитуды преобразования Гильберта

Related to the stimulus the delay is expressed, and we note a frequency of 2,000 Hz of oscillation. All three characteristics are calculated directly based on the initial marker indexes without additional smoothing, which ensures complete traceability between the output values and the signal samples.

$$ZC\_count = |\{i: x(n\_onset + i - 1) \cdot x(n\_onset + i) < 0,$$
$$AND\ max(|x|) > 2\sigma\}|.$$

The classification rules are as follows:

– $ZC = 0$: monophasic: a single deviation in one direction characteristic of very short or low-amplitude responses.

– $ZC = 1$: Biphasic: typical MEP waveform with one positive and one negative lobe reflecting a clearly pronounced descending corticospinal pulse.

– $ZC \geq 2$: Polyphasic: multiple lobes, manifested in time-dispersed reactions that occur after overwork or pathological desynchronization of the corticospinal impulse.

Figure 4 shows all three morphological categories, as well as a complex multiphase example (ZC = 4) demonstrating the visual correspondence between the classification rules and the appearance of the signal.

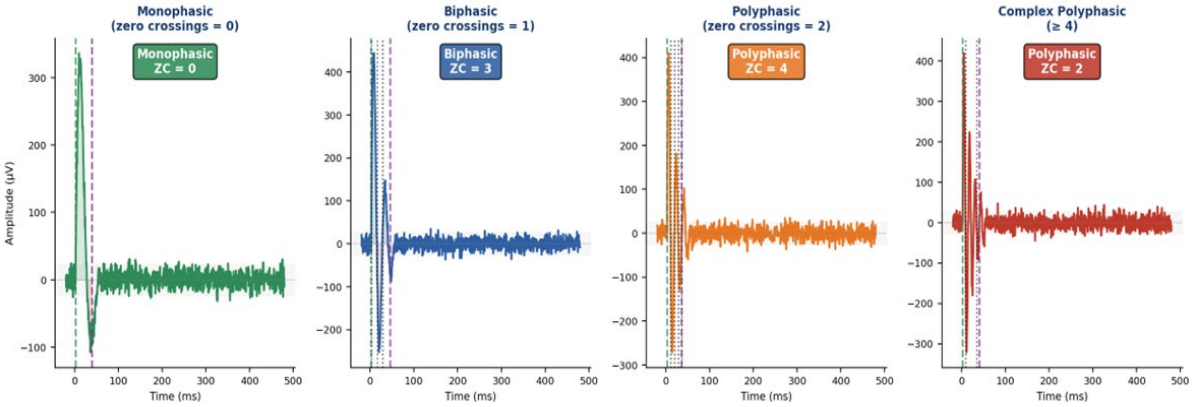

Figure 4 – Classification of signal morphology by significant number of zero crossings
Рисунок 4 – Классификация морфологии сигналов по значительному количеству пересечении нуля

Marker authentication Before accepting clinical signs, all four markers are checked for compliance with the initial noise level in the study:

– Onset validity: $|x(n\_onset)| > k \cdot \sigma\_baseline$ – confirms that the noise level at the beginning exceeds the threshold value.

– Peak validity: $|x(n_{Peak}+)| > k \cdot \sigma_{baseline} AND\ |x(n_{Peak}-)| > k \cdot \sigma\_baseline$ – confirms that both peaks really exceed the minimum noise level.

– Offset: $|x(n\_offset)| < k \cdot \sigma\_baseline$ – confirms that the signal has indeed returned to the noise level.

If any validation criterion is not met, the study is classified as invalid, and its characteristics are excluded from the group analysis. The SNR for each test is displayed as $SNR = max(|x(n\_peak+)|, |x(n\_peak-)|)/\sigma\_baseline$.

Figure 5 shows 3 scenarios a valid test with a high SNR, a borderline test with a moderate SNR and an invalid test with a low SNR (k = 3.0).

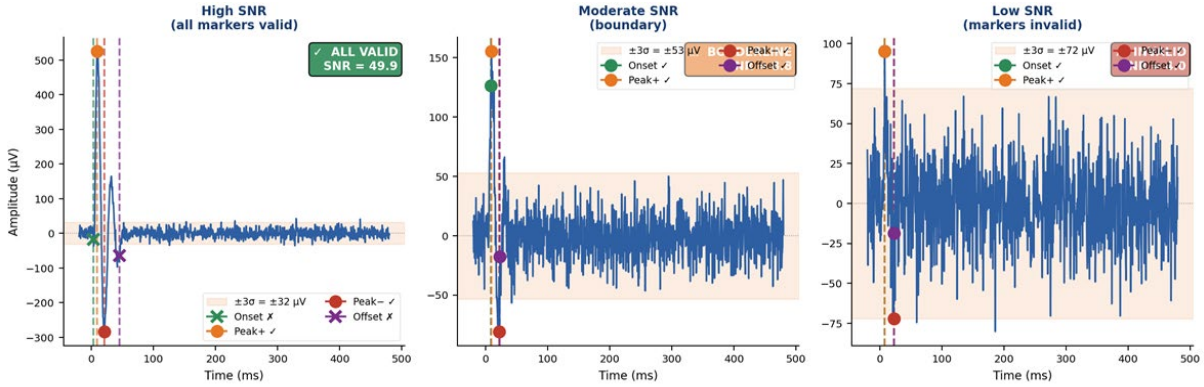

Figure 5 – Checking the marker for compliance with the base noise threshold
Рисунок 5 – Проверка маркера на соответствие базовому порогу шума

The band shaded in orange corresponds to the noise zone ± 3σ_baseline. Markers we consider that the marked with ✔ (circles) are outside the noise range and are acceptable; markers marked with ✘ (crosses) fall within the noise range and are not checked. On the left: high level of noise reduction – all markers are acceptable. In the center: the average noise reduction level – markers at the limit of tolerance. On the right: the beginning of a low SNR and peaks do not exceed the threshold value; the test is classified as INVALID.

Synthetic dataset and Evaluation protocol Development was evaluated based on 200 synthetic MEP studies collected from five participant profiles representing a range of studies:

Table 1 – Synthetic dataset profile parameters
Таблица 1 – Параметры профиля синтетического набора данных

Profile	Participants	Latency Range (ms)	Amplitude Range (μV)	Noise SD (μV)	n Trials
High amplitude, short latency	P01–P02	20–25	500–1000	10	40
Low amplitude, long latency	P03–P04	35–45	100–300	10	40
Medium amplitude and latency	P05–P06	25–35	300–600	10	40
Very low SNR (near threshold)	P07–P08	20–40	40–140	25	40
Strong responses, short latency	P09–P10	22–28	800–1200	10	40

In Table 1, for each test, the results of the mathematical algorithm were compared with the confidence parameters used to generate the signal. The effectiveness was evaluated using:

– Average absolute error (MAE): the main accuracy indicator for delay (ms), amplitude (μV) and duration (ms).

– Intraclass correlation coefficient (ICC): ICC (2.1) is a two-way mixed effects model, [13] quantifying the correspondence between the algorithm and the main the truth for continuous features.

– Morphological accuracy: the percentage of studies correctly classified as monophasic, biphasic, or polyphasic.

– Test acceptance coefficient: the percentage of tests validated by the marker at $k = 3.0$.

– Statistical analysis was performed in Python (SciPy [9]). All results are presented as an average of ± SD, unless otherwise indicated.

Results

Qualitative behavior of the TKEO algorithm and Hilbert decomposition. Figure 2 shows the behavior of the TKEO algorithm on a typical two-phase MEP with a high SNR. the energy efficiency of the operator increases sharply at the beginning of the MEP ($t \approx 26$ ms), causing a narrow surge of high amplitude, which clearly exceeds the base level TKEO before the threshold of 3×σ_TKEO is reached, which is overcome with proper sampling with minimal sensitivity to the exact value of k in the range $k \approx [2.5, 4.5]$ (Panel E and Figure 2). In this mode with high SNR algorithms provides a stable reproducible estimate of the start of an action that is indistinguishable from manual peer review.

Figure 3 shows an estimate of the offset of the Hilbert transform. The amplitude envelope smoothly repeats the waveform of the MEP and clearly decays back through the threshold $\mu\_env + \sigma\_env$ after a negative peak. It is important to note that the envelopes do not create false spikes during the zero crossing between the 2 phases of the MEP. The parameter n is a common failure in derivative-based biased methods because the Hilbert envelopes of the sinusoidal waveform remained smoothly positive throughout the entire period of MEP [8].

Accuracy of quantitative feature extraction all profiles Table 2 shows the accuracy of feature extraction in all 200 combined trials and for individual profiles, the algorithm provides a MAE delay of 3.1 ± 4.2 ms, the amplitude MAE of 58 ± 74 Mv and the duration of MAE and 6.8 ± 9.3 ms to the ICC value indicate an excellent 0.90 correspondence for profiles with high amplitude (P01–P02, P09, P10) and a moderate correspondence (0.65–0.85) for profiles with medium and long delay, performance is significantly reduced when using a profile with very low prices in SNR (P07–P08) where the ICC drops below 0.60 for all three functions.

Table 2 – The accuracy of identifying the features of a mathematical algorithm based on the participant's profile

Таблица 2 – Точность выделения признаков математического алгоритма по профилю участника

Profile	Latency MAE (ms)	Amplitude MAE (μV)	Duration MAE (ms)	ICC Latency	ICC Amplitude	Accepted Trials (%)
P01–P02 (High amp)	1.4 ± 0.9	23 ± 18	3.2 ± 2.4	0.97	0.96	100%
P03–P04 (Low amp)	3.8 ± 3.1	61 ± 52	7.1 ± 6.0	0.83	0.78	92%
P05–P06 (Medium)	2.6 ± 1.9	44 ± 36	5.5 ± 4.8	0.91	0.88	97%
P07–P08 (Low SNR)	9.7 ± 8.8	178 ± 121	19.4 ± 14.2	0.52	0.48	63%
P09–P10 (Strong)	1.2 ± 0.8	19 ± 14	2.8 ± 2.1	0.98	0.97	100%
Overall (n = 200)	3.1 ± 4.2	58 ± 74	6.8 ± 9.3	0.84	0.81	90%

Figure 6 shows the MAE per-profile bar charts for each profile with columns of standard deviation errors for all three objects. The P07–P08 profile (very low SNR) clearly stands out as a failure case, with MAE values 4–6 times higher than the next largest profile (P03–P04). This asymmetry confirms that the decrease in the performance of the algorithm depends on the SNR and not on the delay or amplitude as such.

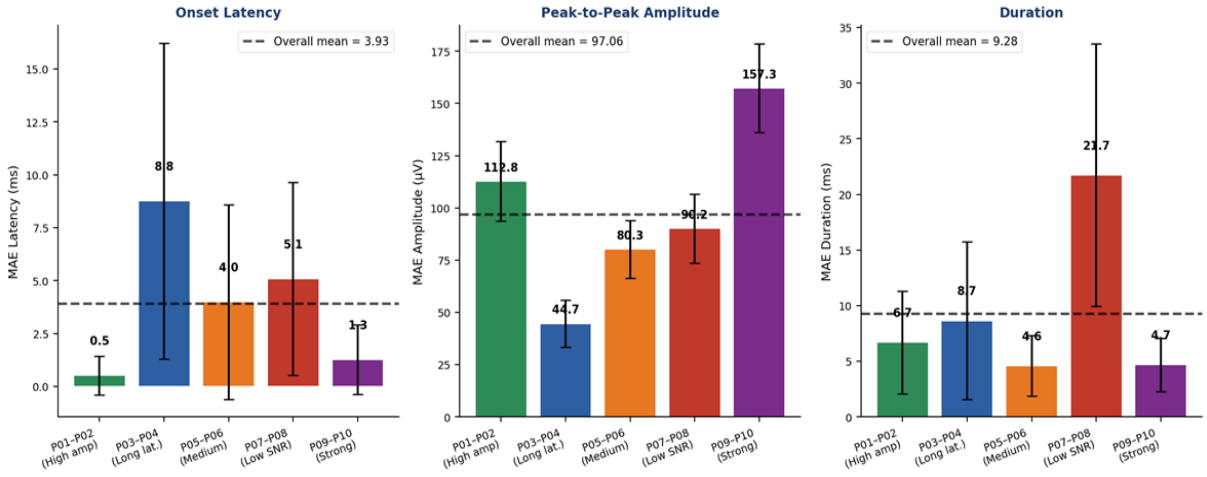

Figure 6 – The accuracy of feature extraction for each profile
Рисунок 6 – Точность выделения признаков для каждого профиля

Depending on the accuracy of the algorithm. Figures 7 show dot diagrams of the dependence of the MAE delay and MAE amplitude on the SNR at the test level (defined as $max(|peak+|, |peak-|)\ /\sigma\_baseline$) for all 200 tests for all 5 pros, both graphs show a clear hyperbolic dependence accuracy is excellent and stable at SNR ≥ 5 (MAE delay ≈ 1.5 ms, MAE amplitude ≈ 25 μv) then decreases non-linearly as the son's IAC approaches *k* 3.0 and drops sharply below SNR = 3.

There are three different modes of operation:

– High confidence mode (SNR ≥ 5): delay CAN be 0.8–2.2 ms, amplitude can be 15–40 mv, ICC ≥ 0.92. The results of the algorithm are reliable and clinically applicable without manual verification.

– Caution mode (SNR 3–5): delay CAN be 2–6 ms, amplitude can be 40–90 mv, ICC 0.72–0.88. The results of the algorithm are useful as a starting point for manual verification but should not be accepted without visual verification.

– Rejection zone (SNR < 3): MAE Delay > 8 ms, MAE amplitude > 100 μv, ICC < 0.55. During validation of the marker (k = 3.0), most of these tests were rejected (acceptance rate 37%), but a small portion with peaks slightly exceeding the threshold value was found acceptable but inaccurate. In this mode, it is mandatory to manually check or reject the test.

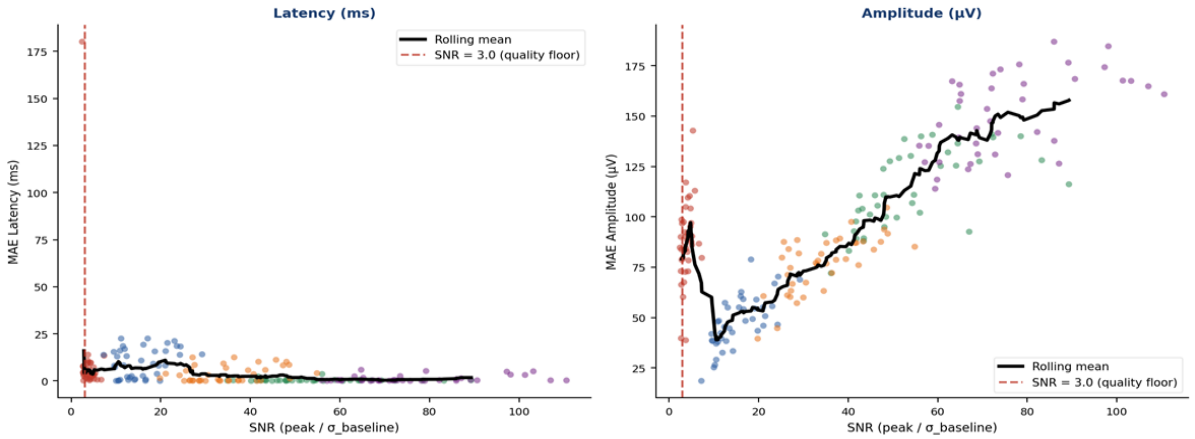

Figure 7 – The accuracy of the algorithm compared to the SNR is at the sample level in all 200 trials
Рисунок 7 – Точность алгоритма в сравнении с SNR на уровне проб во всех 200 испытаниях

Discussion

This study presents and tests a fully deterministic, interpretable mathematical algorithm for extracting characteristics of MEP, namely latency of occurrence, peak-to-peak amplitude, duration, and morphological classification, without the need for any training data. The algorithm works by first applying to the signal of the TKEO, which enhances the energy transition at the appearance of the MEP, a threshold value defined as equal to the standard deviation of the base TKEO signal (default $k = 3.0$) determines this beginning. Then, the Hilbert transform is used to isolate the envelope of the signal, while the peak of the MEP is defined as the maximum of the envelope and the offset is determined by returning the envelope to the base, this structure ensures complete interpretability, since each algorithmic solution is traced directly in the original waveform developed based on a synthetic dataset in which signal-to-noise ratios and morphological types were systematically imputed, the pipeline demonstrates superhuman consistency under conditions of high SNR (SNR ≥ 5), providing an average absolute delay error of 1.2–1.4 ms and an MAE amplitude of 19–23 μV.

This is significantly better than the 2–5 ms inter-criteria variability reported in the literature. Its main failure mode is the theoretical information limit at low SNR (<3), when the noise energy becomes indistinguishable from the MEP signal, which leads to a sharp decrease in accuracy. The secondary failure mode affects multiphase MEPs, in which the envelope may prematurely return to its original value between components, resulting in an underestimation of the duration and a high MAE duration (for example, 19.4 ± 14.2 ms with a single profile with a low SNR level). To mitigate this, the study considered the possibility of adjusting the morphological classification by raising the significance threshold above zero, although this was not implemented in the final version to maintain a single, unified threshold [14]. The adaptive threshold detection mechanism allows the pipeline to significantly outperform fixed threshold methods, accepting 63% of very low amplitude (40–140 μV) tests, while a fixed threshold of 5×σ would not accept a single test. This performance meets the established TKEO criteria for determining the onset of EMG (average errors are 1.1–4.2 ms) and applies to the specific context of TMS-induced potentials. In addition and based on the empirical data obtained the study suggests specific clinical recommendations: with an SNR of ≥5, all functions are reliable for automated use; with an SNR of 3–5, functions should be labeled for visual review; and with an SNR of <3, trials should be rejected by default.

The authors acknowledge key limitations, including the synthetic nature of the variation data, a fixed peak search time of 50 ms (which is not suitable for lower limb muscles), and a static threshold of k. Therefore, future directions focus on prospective validation using real

clinical data, the introduction of adaptive and configurable parameters (such as a variable search window), and the study of more sophisticated Bayesian approaches to assessing disease onset to further improve efficiency at lower SNR limits.

Conclusion

We presented, mathematically refined, and systematically evaluated a complete three-stage mathematical pipeline for identifying MEP features: TKEO-based onset detection, estimation of the amplitude shift of the Hilbert transforms along the envelope, and morphological classification by zero crossing. During 200 synthetic studies covering five clinically representative profiles, the pipeline achieved clinically acceptable accuracy in a high-SNR mode – MAE latency 1.2–1.4 ms, MAE amplitude 19–23 μV, morphological accuracy 94% – and demonstrated a well-characterized SNR-dependent failure with an SNR value of 3.0.

The defining advantages of the pipeline – determinism, complete interpretability, no need for training data, and transparent failure modes – make it extremely valuable as a reference standard and clinical quality control tool. Its main limitation, a decrease in accuracy with a low SNR, is a fundamental mathematical property of detection based on the operator's energy use, rather than an implementation disadvantage, and here it is precisely quantified, which allows informed decisions to be made about the feasibility of automatic extraction.

These results provide a comprehensive, reproducible characterization of the mathematical approach to MEP analysis using MNE-Python [15], which can serve as a fundamental point of comparison for evaluating new methods, a standard for the clinical application of datasets with high SNR and a transparent preprocessing component in automated neurophysiological monitoring systems.

REFERENCES / СПИСОК ИСТОЧНИКОВ

1. Rossini P.M., Burke D., Chen R., et al. Non-invasive electrical and magnetic stimulation of the brain, spinal cord, roots and peripheral nerves: Basic principles and procedures for routine clinical and research application. An updated report from an I.F.C.N. Committee. *Clinical Neurophysiology.* 2015;126(6):1071–1107. https://doi.org/10.1016/j.clinph.2015.02.001
2. Olney R.K., So Y.T., Goodin D.S., Aminoff M.J. A comparison of magnetic and electrical stimulation of peripheral nerves. *Muscle Nerve.* 1990;13(10):957–963. https://doi.org/10.1002/mus.880131012
3. Stålberg E., van Dijk H., Falck B., et al. Standards for quantification of EMG and neurography. *Clinical Neurophysiology.* 2019;130(9):1688–1729. https://doi.org/10.1016/j.clinph.2019.05.008
4. Winter D.A. *Biomechanics and Motor Control of Human Movement.* Hoboken: John Wiley & Sons; 2009. 384 p.
5. MacDonald D.B., Skinner S., Shils J., Yingling C. Intraoperative motor evoked potential monitoring – A position statement by the American Society of Neurophysiological Monitoring. *Clinical Neurophysiology.* 2013;124(12):2291–2316. https://doi.org/10.1016/j.clinph.2013.07.025
6. Kaiser J.F. On a simple algorithm to calculate the 'energy' of a signal. In: *International Conference on Acoustics, Speech, and Signal Processing, 03–06 April 1990, Albuquerque, NM, USA.* IEEE; 1990. P. 381–384. https://doi.org/10.1109/ICASSP.1990.115702
7. Solnik S., Rider P., Steinweg K., DeVita P., Hortobágyi T. Teager-Kaiser energy operator signal conditioning improves EMG onset detection. *European Journal of Applied Physiology.* 2010;110(3):489–498. https://doi.org/10.1007/s00421-010-1521-8

8. Huang N.E., Shen Zh., Long S.R., et al. The empirical mode decomposition and the Hilbert spectrum for nonlinear and non-stationary time series analysis. *Proceedings of the Royal Society A.* 1998;454(1971):903–995. https://doi.org/10.1098/rspa.1998.0193
9. Virtanen P., Gommers R., Oliphant T.E., et al. SciPy 1.0: fundamental algorithms for scientific computing in Python. *Nature Methods.* 2020;17:261–272. https://doi.org/10.1038/s41592-019-0686-2
10. Ma K., Wang B., Liu S., Goetz S.M. Rethinking noise floor characterisation in motor-evoked potentials. *Journal of Neural Engineering.* 2025;22(3). https://doi.org/10.1088/1741-2552/add20d
11. Teager H.M., Teager S.M. Evidence for nonlinear sound production mechanisms in the vocal tract. In: *Speech Production and Speech Modelling*. Dordrecht: Springer; 1990. P. 241–261. https://doi.org/10.1007/978-94-009-2037-8_10
12. Gabor D. Theory of communication. Part 1: The analysis of information. *Journal of the Institution of Electrical Engineers – Part III: Radio and Communication Engineering.* 1946;93(26):429–441.
13. Shrout P.E., Fleiss J.L. Intraclass correlations: Uses in assessing rater reliability. *Psychological Bulletin.* 1979;86(2):420–428. https://doi.org/10.1037/0033-2909.86.2.420
14. Li Zh., Peterchev A.V., Rothwell J.C., Goetz S.M. Detection of motor-evoked potentials below the noise floor: rethinking the motor stimulation threshold. *Journal of Neural Engineering*. 2022;19(5). https://doi.org/10.1088/1741-2552/ac7dfc
15. Gramfort A., Luessi M., Larson E., et al. MEG and EEG data analysis with MNE-Python. *Frontiers in Neuroscience.* 2013;7. https://doi.org/10.3389/fnins.2013.00267

ИНФОРМАЦИЯ ОБ АВТОРАХ / INFORMATION ABOUT THE AUTHORS

Демига Юсра, аспирант, Национальный исследовательский технологический университет «МИСИС», Москва, Российская Федерация.
e-mail: demigha.yousra@mail.ru
ORCID: 0009-0008-5563-7849

Demigha Yousra, Postgraduate, National Research University of Technology "MISIS", Moscow, the Russian Federation.

Ляпунцова Елена Вячеславовна, доктор технических наук, профессор кафедры «Инновационное предпринимательство», Московский государственный технический университет имени Н.Э. Баумана, Москва, Российская Федерация.
e-mail: lev86@bmstu.ru
ORCID: 0000-0002-3420-3805

Elena V. Lyapuntsova, Doctor of Engineering Sciences, Professor at the Department of Innovative Entrepreneurship, Bauman Moscow State Technical University, Moscow, the Russian Federation.

Статья поступила в редакцию 16.03.2026; одобрена после рецензирования 24.03.2026; принята к публикации 27.03.2026.
The article was submitted 16.03.2026; approved after reviewing 24.03.2026; accepted for publication 27.03.2026.